

First-Principles Study of the Optical Properties of SrHfO₃

H. Salehi, H. Tolabinejad

Department of Physics, Shahid Chamran University of Ahvaz, Ahvaz, Iran

E-mail: salehi_h@scu.ac.ir

Received March 17, 2011; revised April 15, 2011; accepted April 25, 2011

Abstract

The optical properties of SrHfO₃ were studied by first principle using the density functional theory. The dielectric functions and optical constants are calculated using the full potential—linearized augmented plane wave (FP-LAPW) method with the generalized gradient approximation (GGA) by Wien2k package. The theoretical calculated optical properties and energy loss (EEL) spectrum yield a static refractive index of 1.924 and a Plasmon energy of 27 eV for cubic phase. The complex dielectric functions are calculated which are in good agreement with the available experimental results.

Keywords: Optical Properties, SrHfO₃, WIEN2k, FP-LAPW, DFT, GGA

1. Introduction

The development of computational methods in the electronic-structure community has led to a new class of first principles approaches, based upon a full solution of the quantum mechanical ground state of the electron system within the local-density approximation (LDA) to Kohn-Sham density functional theory (DFT) [1,2]. In principle, these methods take as their only inputs the atomic numbers of the constituent atoms. The modeling of electronic and optical properties, by means of first-principles calculations, has become a very useful tool for understanding about the structural, electronic and optical properties of the various materials.

A particularly successful application of this technique has been its use in understanding the Perovskite ferroelectric Compounds. SrHfO₃ is a typical perovskite dielectric with a wide range of technological applications. Because of its special properties related to ferroelectricity, semi conductivity. SrHfO₃ is a Compound that has a Composition and lattice structure similar to SrTiO₃. Although the perovskite Compound SrHfO₃ has been well known for a long time, theoretical studies on this compound are few [3]. Material with structure ABO₃ have been the subject of extensive investigation, because of the unusual combination of their magnetic, electronic and transport properties [4,5]. Their use in technological applications is also diverse, including optical wave guides, laser-host crystals, high temperature oxygen sensors, high-voltage capacitor, piezoelectric materials in actuators and so on [6,7]. Recently, Stachiotti *et al.* [8] inves-

tigated its ferroelectric instability by first-principles calculation. First-Principles calculation is one of the powerful tools for carrying out the theoretical studies of the electronic and structure properties of materials. The ABO₃ Perovskite type oxides have potentials to be attractive functional materials because of their various unique Properties. Among them, alkaline earth rare-earth hafnates, (AHfO₃, A = Ba, Sr or Ca) have been reported [3,9] as promising Candidates as scintillators used in γ -ray imaging fields, such as positron emission tomography. Besides, SrHfO₃ is a promising candidate high-k dielectric oxide for the next generation of CMOS devices, due to its good physical and electrical Properties [10].

Kennedy *et al.* [11] concluded that SrHfO₃ undergoes three phase transitions: From 300 K to approximately 670 K the structure of SrHfO₃ is orthorhombic with space group Pnma. By 870 K it adopts a second orthorhombic structure with space group Cmc21. It then undergoes a further phase transition and is tetragonal with space group I4/mcm from 1000 to 1353 K. At higher temperature the structure is the ideal cubic perovskite with space group Pm $\bar{3}$ m. In the present work the optical properties of SrHfO₃ in cubic phase have been studied using the FP-LAPW method. The results, in comparison with the previous theoretical data, are in better agreement with the experimental results.

2. Method of Calculation

Calculation of the optical properties of SrHfO₃ were carried out with a self-consistent scheme by solving the

Kohn-Sham Equation using aFP-LAPW method in the framework of theDFT along with the GGA method [12, 13] by WIEN2k package [14]. In the FP-LAPW method, space is divided into two regions, a spherical “muffin-tin” around the nuclei in which radial solutions of Schrödinger Equation and their energy derivatives are used as basis functions, and an “interstitial” region between the muffin tins (MT) in which the basis set consists of plane waves. There is no pseudopotential approximation and core states are calculated self-consistently in the crystal potential. Also, core states are treated fully relativistically while valence and semi-core states are treated semi-relativistically (*i.e.* ignoring the spin-orbit coupling). The cut-off energy, which defines the separation of the core and valence states, was chosen as -6 Ry. The complex dielectric tensor was calculated, in this program, according to the well-known relations [15].

$$\text{Im } \varepsilon_{\alpha\beta}(\omega) = \frac{4\pi e^2}{m^2 \omega^2} \sum_{c,v} \int dk \langle c_k | p^\alpha | v_k \rangle \langle v_k | p^\beta | c_k \rangle \delta(\varepsilon_{c_k} - \varepsilon_{v_k} - \omega) \quad (1)$$

$$\text{Re } \varepsilon_{\alpha\beta}(\omega) = \delta_{\alpha\beta} + \frac{2}{\pi} P \int_0^\infty \frac{\omega' \text{Im } \varepsilon_{\alpha\beta}(\omega')}{\omega'^2 - \omega^2} d\omega' \quad (2)$$

And the optical conductivity is given by:

$$\text{Re } \sigma_{\alpha\beta}(\omega) = \frac{\omega}{4\pi} \text{Im } \varepsilon_{\alpha\beta}(\omega) \quad (3)$$

In Equation (1), c_k and v_k are the crystal wave functions corresponding to the conduction and the valence bands with crystal wave vector \mathbf{k} . In Equation (3) the conductivity tensor relating the interband current density j in the direction which flows upon application of an electric field E in direction in which the sum in Equation (1) is over all valence and conduction band states labeled by v and c . Moreover, the complex dielectric constant of a solid is given as:

$$\varepsilon(\omega) = \varepsilon_1(\omega) + i\varepsilon_2(\omega) \quad (4)$$

Here, real and imaginary parts are related to optical constants $n(\omega)$ and $k(\omega)$ as:

$$\begin{aligned} \varepsilon_1(\omega) &= n^2(\omega) - k^2(\omega) \\ \varepsilon_2(\omega) &= 2n(\omega)k(\omega) \end{aligned} \quad (5)$$

The other optical parameters, such as energy-loss spectrum and oscillator strength sum rule are immediately calculated in terms of the components of the complex dielectric function [15].

3. Results and Discussion

The calculations first were carried out using the experimental data for lattice constants ($a = 7.78$ a.u) [8] in the

cubic phase. Then by minimizing the ratio of the total energy of the crystal to its volume (volume optimizing) the theoretical lattice constants were obtained ($a = 7.87$ au). In order to reduce the time of the calculations we used the symmetries of the crystal structure and some other approximations for simplicity. The calculation was performed with 1000 k-points in the cubic phase.

The self-consistent process, for both phases, after 11 cycles had convergence of about 0.0001 in the eigenvalues in which for the cubic phase 388 plane waves were produced. Under these conditions the values of the other parameters were $G_{\max} = 14$, $R_{\text{MT}}(\text{Sr}) = 2$ au, $R_{\text{MT}}(\text{Hf}) = 2.2$ au, $R_{\text{MT}}(\text{O}) = 1.5$ au. The iteration halted when the total charge adjustment was less than 0.0001 between steps.

3.1. Dielectric Function

In WIEN2K calculations for finding optical functions, reflections of kramers-kronig was used. As an example in transformation kramers-kronig, without coupling spin-orbit and magnetic field, the dielectric tensor cubic structure is as follows:

$$\left(\begin{array}{ccc} \text{Im } \varepsilon_{xx} & 0 & 0 \\ 0 & \text{Im } \varepsilon_{xx} & 0 \\ 0 & 0 & \text{Im } \varepsilon_{xx} \end{array} \right) \left. \vphantom{\begin{array}{ccc} \text{Im } \varepsilon_{xx} & 0 & 0 \\ 0 & \text{Im } \varepsilon_{xx} & 0 \\ 0 & 0 & \text{Im } \varepsilon_{xx} \end{array}} \right\} \text{kramers - kronig} \quad (6)$$

$$\left(\begin{array}{ccc} \text{Re } \varepsilon_{xx} & 0 & 0 \\ 0 & \text{Re } \varepsilon_{xx} & 0 \\ 0 & 0 & \text{Re } \varepsilon_{xx} \end{array} \right)$$

In this theoretical method, momentum matrix elements, for finding dielectric function and other optical properties Equation (3) is used. Because it has hexagonal closed packed structure (hcp), so due to tensor form for this structure, the selections ε_{xx} (dielectric function in direction x) and ε_{zz} (dielectric function in direction z) are enough for calculating dielectric tensor.

We calculated optical properties of SrHfO_3 in the cubic phase. The real and the imaginary parts of the dielectric functions are shown in **Figure 1** for SrHfO_3 in the cubic phase. In Figure, there are mainly four peaks (5.5, 7, 9.5 and 12 eV). Peaks A (5.5 eV), B(7 eV) correspond mainly to the transitions from O 2p to Hf 5d states along the Γ direction, and peaks C(9.5 eV), D(12 eV) correspond mainly to the transitions from semicore bands (formed by Sr- 4p and O- 2s states) to conduction bands. The value of the main peak of $\varepsilon_1(\omega)$ curve is 6 at energy of 5.5 eV and for $\varepsilon_2(\omega)$ is 6.4 at the energy equal 4 eV.

Figure 1 shows the change of $\text{Re}(\varepsilon_{xx})$ (Real part of dielectric function in the x direction) against photons

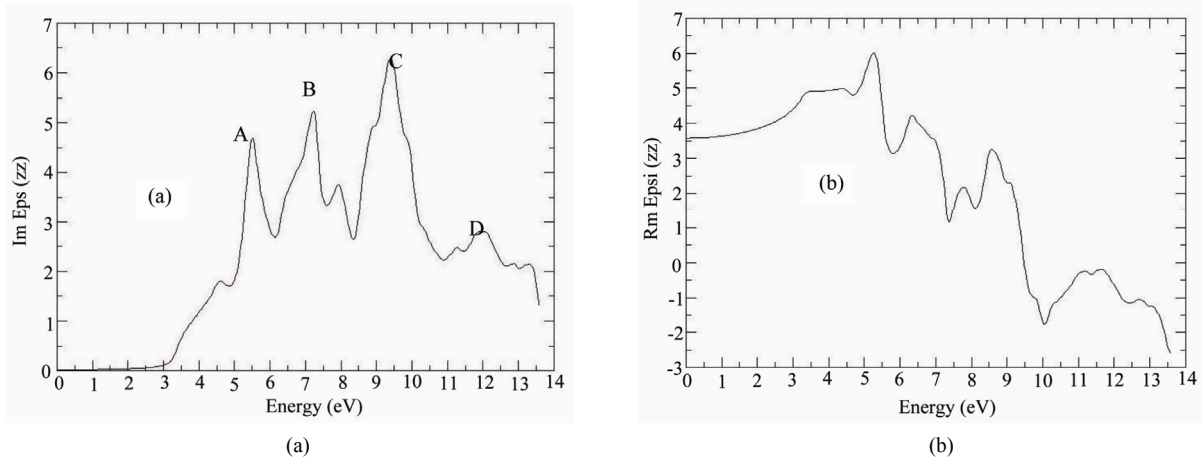


Figure 1. (a) Real and (b) imaginary part of the dielectric function for SrHfO₃ in cubic phase.

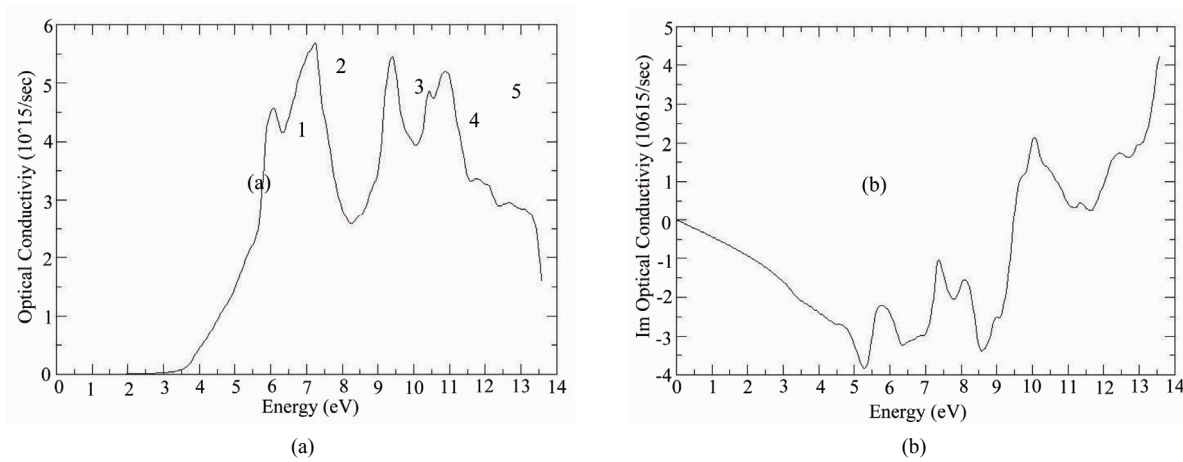


Figure 2. (a) Real and (b) imaginary part of the optical conductivity for SrHfO₃ in cubic phase.

Table 1. SrHfO₃ static refractive index in cubic phase calculated by various methods.

	Present work			Other work
	FP-LAPWG GA96	FP-LAPWG GA91	FP-LAP-WLDA	Experimental [16]
Refractive index (n)	1.924	1.9050	1.867	2
Difference with exp. (%)	3.8	4.75	6.65	-
	3.7	3.63	3.5	4

energy. In the zero energy level, the magnitude of dielectric function, $\epsilon(0)$ is equal to 3.7. By the relation $\sqrt{\epsilon(\omega)} = n(\omega) + ik(\omega) = N(\omega)$, the root of dielectric function will give the refraction coefficient of SrHfO₃ which is equal to $n = \sqrt{\epsilon(0)} = \sqrt{3.7} = 1.924n$. The magnitude of experimental refraction coefficient for

SrHfO₃ is 2 [16] which has a good agreement.

The first peak of $\text{Im } \epsilon$ is contributed to transition from the upper valence bands to the lower conduction band. Our calculated in direct ($\Gamma-R$) band gap of SrHfO₃ is about 3.7 eV.

The real part of the dielectric function ($\text{Re } \epsilon$) follow from the Kramer-kronig relationship. All Optical constant may be derived from this.

Referring to **Table 1**, it can be seen that the calculated refractive index in this work is in agreement with experimental results.

3.2. Optical Conduction

The real and the imaginary parts of optical conductivity are shown in **Figure 2** for SrHfO₃ in cubic phase.

In this theoretical method, momentum matrix elements is used for finding dielectric function and other optical properties. Also we have used transformation Kramers-Kronig for calculating real part dielectric tensor.

Notice that, occupied electron states are excited to unoccupied electron states in upper Fermi level by absorbing photons. This interband transition is called optical conduction (also called Drude transition) and photon absorption by electron is called interband absorption.

Figure 4 shows the change of real part of optical conduction (in 10^{15} s^{-1}) in the X direction with respect to internal photon energy. As in the **Figure 2**, the optical conduction starts with energy of about 2eV and by increasing photon energy, the optical conduction will rise and in the range of 6.5 till 7 eV, will reach to the upper level. The reason of starting optical conduction, $\sigma(\omega)$, from 2eV energy, is the gap of energy. So the excited electrons have no enough energy to pass the energy gap, and transfer to the conduction band.

For the absorption coefficient, $\alpha(\omega)$, the absorption edge start from about 3.4 eV, corresponding to the direct $\Gamma - \Gamma$ transition. The maximum reflectivity about 13eV, ie the minimum value ε_1 will occur. In the regime incident beam energy, has not been reached to create a new exaction mode yet or can prepar interband transition and thus waves will be completely reflectivity.

The peak function $\alpha(\omega)$ also in energy 11.5 eV can be seen, and with this mean the most value absorption in the band gap, which the matter cannot exhibit any transparency.

In **Figure 3** the optical parameters is shown for SrHfO_3 in cubic phase. The static refractive index value for SrHfO_3 in the cubic phase calculated in this work, and the values obtained by other methods are summarized in **Table 1**.

If we assume orientation of the crystal surface parallel to the optical axis, the reflectivity $R(\omega)$ follows directly from Fresnel's formula.

$$R(\omega) = \left| \frac{\sqrt{\varepsilon(\omega)} - 1}{\sqrt{\varepsilon(\omega)} + 1} \right|^2 \quad (7)$$

Expression for the absorption coefficient $I(\omega)$ now follow:

$$I(\omega) = \sqrt{2}(\omega) \left(\sqrt{\varepsilon_1(\omega)^2 + \varepsilon_2(\omega)^2} - \varepsilon_1(\omega) \right)^{1/2} \quad (8)$$

3.3. Electron Energy Loss Spectroscopy

EELS is a valuable tool for investigating various aspects of materials. It has the advantage of covering the complete energy range including non-scattered and elastically

scattered electrons (Zero Loss). At intermediate energies (typically 1 to 50 eV) the energy losses are due primarily to a complicated mixture of single electron excitations and collective excitations (plasmons). The positions of the single electron excitation peaks are related to the joint density of states between the conduction and valence bands, whereas the energy required for the excitation of bulk plasmons depends mainly on the electron density in the solid. Here electrons, which excite the atoms electrons of the outer shell is called Valence Loss or valence interband transitions. At higher energies, typically a few hundred eV, edges can be seen in the spectrum, indicating the onset of excitations from the various inner atomic shells to the conduction band. In this case the fast electrons excite the inner shell electrons (Core Loss) or induce core level excitation of Near Edge Structure (ELNES) and XANES. The edges are characteristic of particular elements and their energy and height can be used for elemental analysis.

In the case of interband transitions, which consist mostly of plasmon excitations, the scattering probability for volume losses is directly connected to the energy loss function. One can then calculate the EEL spectrum from the following relations.

$$\varepsilon_{\alpha\beta}(\omega) = \varepsilon_1 + i\varepsilon_2 \quad \text{and} \quad \text{EELSpectrum} = \text{Im}[-1/\varepsilon_{\alpha\beta}(\omega)] = \frac{\varepsilon_2}{\varepsilon_1^2 + \varepsilon_2^2} \quad (9)$$

These peaks can, however, have different origins such as charge carrier plasmons and interband or intraband excitations. The energy of the maximum peak of $\text{Im}[-\varepsilon^{-1}(E)]$ at 27 eV is assigned to the energy of the volume plasmon $\hbar\omega_p$. The first peak at 9 eV and second peak at 13eV originates from O-2p to Hf-3d and Sr-p orbitals, respectively **Figure 4**. The value of $\hbar\omega_p$ obtained in this work and for free electron is given in **Table 3**.

For free electrons the plasmon energy is calculated according to the following model:

$$\hbar\omega_p^e = \hbar \sqrt{\frac{ne^2}{\varepsilon_0 m}} \quad (10)$$

If we use this model, then what should be the number of valance electrons per SrHfO_3 molecule, N, used to calculate the density of valance electrons, n, and thus the plasmon energy in Equation (7). If we take only the contribution of $4s^2$, $4p^6$ and $5s^2$ electrons of Sr, $5s^2$, $5p^6$, $5d^{10}$ and $6s^2$ of Hf and $2s^2$, $2p^4$ of O (ignoring the contribution of $5s^2$ and $2s^2$ electron of Sr and O atom respectively) and the free and electron plasmon energy will be 31eV. Otherwise, with all valance electrons of Sr, Hf and O atoms, the free electron plasmon would be 38.6eV. We will also see from sum rule is a reasonable value for the valance electrons per SrHfO_3 molecule.

Table 2. The value transition interband.

Transition	First	Two	Three	Four	Five
E(eV)	5.5	6.7	9.5	10.5	11.2

Table 3. SrHfO₃ plasmon energy ($\hbar\omega_p$) of the energy loss function in cubic phase calculated by this method and free electron.

	Present work	Present work	Present work	Present work	Present work	Other work
	GGA96	GGA91	LDA	Free electron (ignoring Sr-5s and O-2s states)	Free electron	Theoretical [17]
Plasmon energy (eV)	27	27.73	26.2	31	38.6	27.3

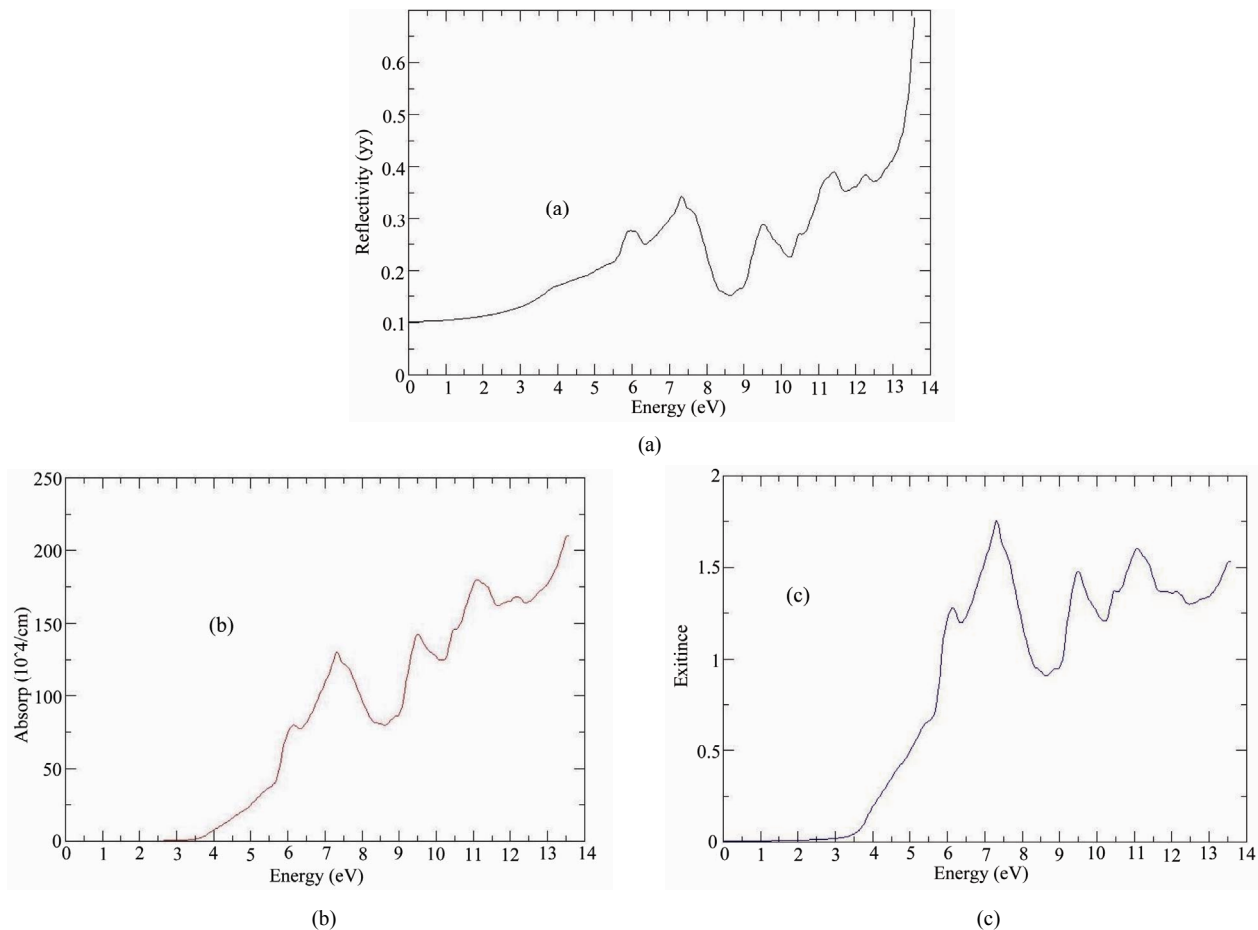


Figure 3. The calculated optical parameters of the cubic SrHfO₃ as a function of the photon energy (eV). (a), absorption coefficient, $\alpha(\omega)$; (b), reflectivity coefficient $R(\omega)$ and (c), extinction coefficient $k(\omega)$.

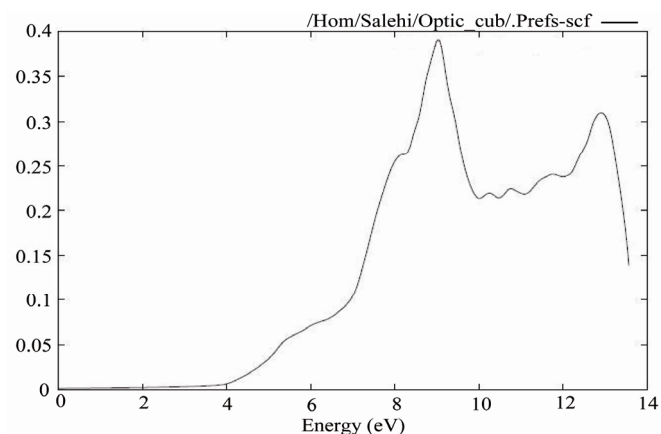


Figure 4. Electron energy Loss spectroscopy for SrHfO₃ cubic phase.

4. Conclusions

We have calculated the optical properties of SrHfO₃ in cubic phases using the FP-LAPW method with the generalized gradient approximation (GGA). The calculations show a static refractive index of 1.924 and an EEL spectrum of 27eV for the cubic phase. Ignoring the contribution of 5s² and 2s² electron of Sr and O atom respectively, the free electron plasmon energy will be 38.6 eV. It seems that is a reasonable value for the valance electrons per molecule. The calculated results show a good agreement with the other data.

5. References

- [1] J. P. Perdew, J. A. Chevary, *et al.*, *Phys.Rev.B*, Vol. 46, No. , 1992, pp. 6671-6687.
- [2] J. P. Perdew, *Physical. B*, Vol. 172, No. , 1991, pp. 1-6.
- [3] Y. M. Ji, D. Y. Jiang, Z. H. Wu, T. Feng and J. L. Shi, *Mater.Res.Bull.*, Vol. 40, No. , 2005, pp. 1521
- [4] I. R. Shein, V. L. Kozhevnikov and A. L. Ivanovskii, *Solid State Sci.* Vol.10, No. , 2008, pp. 217.
- [5] C. M. I. Okoye, *J. Phys.: Condens. Matter*, Vol. 15, No. , 2003, pp. 5945.
- [6] S. Lin, Z. Xiu, J. Liu, F. Xu, W. Yu, J. Yu and G. Feng, *J. Alloy. Compd*, Vol. 457, No. , 2008, pp. L12.
- [7] V. M. Longo, L. S. Cavalcante, A. T. de Figueiredo, L. P. Santos, E. Longo, J. A. Varela, J. R. Sambrano, C. A. Paskocimas, F. S. De Vicente and A. C. Hernandez, *Appl. Phys. Lett.* Vol. 90, No. , 2007, pp. 091906.
- [8] M. G. Stachiotti, G. Fabricius, R. Alonso and C. O. Rodriguez, *Phys.Rev.B*, Vol. 58, No. , 1998, pp. 8145.
- [9] R. Vali, *Solid State Communications*, Vol. 148, No. , 2008, pp. 29-31.
- [10] C. Rossel, M. sousa, C. Marchiori, *et al. Microelec. Eng* Vol. 84, No. , 2007, pp. 1869.
- [11] B. J. Kennedy, C. J. Howard and B. C. Chakoumakos, *Phys.Rev.B*, Vol. 60, No. , 1999, pp. 2972.
- [12] J. P. Perdew, J. A. Chevary, S. H. Vosko, K. A. Jackson, M. R. Pederson, D. J. Singh and C. Fiolhais, *Phys. Rev. B* Vol. 46, No. , 1992, pp. 6671-6687.
- [13] M. Peterson, F. Wanger, L. Hufnagel, M. Scheffler, P. Blaha and K. Schwarz, *Computer Physics Communications*, 126, (2000) 294-309.
[doi:10.1016/S0010-4655\(99\)00495-6](https://doi.org/10.1016/S0010-4655(99)00495-6)
- [14] P. Blaha and K. Schwarz, *WIEN2k*, Vienna University of Technology Austria, 2009.
- [15] F. Wooten, "Optical Properties of Solids," Academic Press, New York, 1972.
- [16] M. Sousa, C. Rossel, C. Marchiori, D. Caimi, J. P. Locquet, D. J. Webb, K. Babich, J. W. Seo and C. Dieker, *J. Appl. Phys.* Vol. 102, No. , 2007, pp. 104103.
- [17] Z. Feng, H. ShouxinCui and C. HengshuaiLi, *Journal of Physics and Chemistry of Solids* Vol. 70 No. , 2009, pp. 412-416.